

Atomic-Scale Friction on Stepped Surfaces of Ionic Crystals

Pascal Steiner,¹ Enrico Gnecco,^{2,*} Franciszek Krok,³ Janusz Budzioch,³ Lukasz Walczak,³ Jerzy Konior,³ Marek Szymonski,³ and Ernst Meyer¹

¹*Department of Physics, University of Basel, Klingelbergstrasse 82, 4056 Basel, Switzerland*

²*IMDEA Nanoscience, Campus Universitario de Cantoblanco, Avenida Francisco Tomás y Valiente 7, 28049, Madrid, Spain*

³*Research Centre for Nanometer Scale Science and Advanced Materials (NANOSAM), Institute of Physics, Jagiellonian University, Reymonta 4, 30-059 Krakow, Poland*

(Received 13 December 2010; published 6 May 2011)

We report on high-resolution friction force microscopy on a stepped NaCl(001) surface in ultrahigh vacuum. The measurements were performed on single cleavage step edges. When blunt tips are used, friction is found to increase while scanning both up and down a step edge. With atomically sharp tips, friction still increases upwards, but it decreases and even changes sign downwards. Our observations extend previous results obtained without resolving atomic features and are associated with the competition between the Schwöbel barrier and the asymmetric potential well accompanying the step edges.

DOI: 10.1103/PhysRevLett.106.186104

PACS numbers: 68.35.Af, 07.79.Sp, 68.35.Ct, 81.65.Cf

Measuring the friction forces acting on an atomically sharp tip sliding across a well-defined obstacle (such as a monatomic step edge) is quite important for a better understanding of mechanical processes occurring on the nanometer scale. A common observation in the few experimental studies on this topic [1–5] is the enhancement of friction at step edges, which is attributed to the activation barriers for diffusion at such locations (*Schwöbel-Ehrlich barriers*) [6,7]. Indeed, in the investigations reported so far, friction was usually found to increase when a step edge was crossed both upwards and downwards, although the friction variation may be not always appreciable in the step-down direction [1,5]. It is important to note that all these studies were performed on length scales in the micrometer range, with no atomic resolution along the scan direction.

In this Letter, we have used an atomic force microscope (AFM) in contact mode to scan cleavage step edges on a NaCl(001) surface in ultrahigh vacuum (UHV). When the tip climbs up an edge, the latter always acts as an obstacle, increasing the friction force experienced by the tip. However, when the tip crosses the edge downwards, two different tendencies are observed. Blunt tips are still pinned—and friction consequently increases—as upwards. Atomically sharp tips, in contrast, easily slip into the bottom of the edge, thus experiencing a friction force which is temporarily oriented in the direction of motion and not opposite to it. This behavior seems to contradict the presence of a strong Schwöbel barrier.

Our measurements were performed with a home-built AFM setup at a pressure of about 10^{-10} mbar [8]. The NaCl(001) surface was cleaved in UHV and annealed at 150 °C to remove surface charges. The results presented below were obtained with a commercial cantilever with normal resonance frequency $f_{\text{norm}} = 10.8$ kHz and stiffness $k_{\text{norm}} = 0.117$ N/m (Nanosensors, PPP-CONT).

The (lateral) friction force F was detected by using a four quadrant photodiode, which is sensitive to the cantilever torsion. In order to calibrate the normal and lateral forces, we used the method discussed in Ref. [9].

Figures 1(a) and 1(b) show a topography and the corresponding lateral force image acquired on a 15×15 nm² area across a step edge of NaCl(001) with one monolayer height. The normal force was kept constant at the value $F_N = -0.2$ nN, assuming that $F_N = 0$ corresponds to the unbent cantilever. As shown by the arrow in Fig. 1(a), some kink sites are present. The most noticeable feature are the atomic features revealed across the step edge. This is clearly visible also in the profile in Fig. 1(c), where the surface height drops 0.22 nm (slightly less than half of lattice constant $a = 0.564$ nm) within 0.28 nm. Furthermore, the change of contrast in both images suggests that the tip apex has a width of two lattice constants in the fast scan direction. Since the measurements were performed a few days after cleaving the NaCl surface, many atomic defects are present. As shown by the circle in Fig. 1(b), the defects always appear as squares with side length $2a$, meaning that the tip end has a width of two lattice constants also in the slow scan direction. Furthermore, the lateral force profiles for the forward and backward scans are almost overlapping, and the friction loop is consequently quite small. This means that the measurements were performed close to the superlubric transition [10]. For the scan in the step-up direction (continuous curve), friction increases at the step edge as expected. In contrast, the lateral force for the step-down direction (dashed curve) decreases and changes sign when crossing the edge, meaning that the tip temporarily overtakes the cantilever.

Although images like those presented in Fig. 1 could be reproduced with different cantilevers, they still represent an exception rather than the rule. Figure 2 shows a topography and a friction map acquired across another step edge.

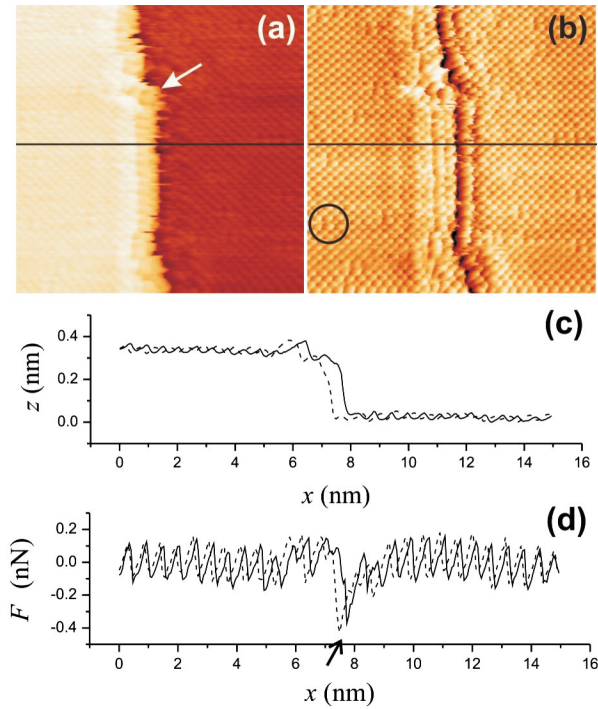


FIG. 1 (color online). (a) AFM topography image (frame size: $15 \times 15 \text{ nm}^2$) and (b) corresponding lateral force image acquired across a single cleavage step edge on a NaCl(001) surface by using a load of -0.2 nN . A kink site is highlighted in (a) by a white arrow, whereas the circle in (b) points out a defect. Profiles are taken along the black line for (c) the topography and (d) the lateral force for the forward scan direction (continuous curves). The dashed profiles represent the backward scan direction (images not shown). The arrow indicates that friction increases step-up (dashed curve) but decreases step-down (continuous curve).

Here we used the same tip as in Fig. 1 after repeated scanning with high loads in different regions on the surface. The horizontal traces clearly indicate the presence of abrasion wear, which contaminates the tip and increases the size of the contact area between the tip and surface [11]. The friction profiles in the two directions also changed considerably. Friction is now enhanced in both directions when the tip crosses the step edge. Images taken with other blunt tips presented similar features. Incidentally, we have also tried to excite the normal and torsional resonance of the cantilever while scanning, which is expected to reduce friction [12,13]. Although this has indeed been the case, the resolution of the AFM images across the step edge could not be improved in such a way.

Friction on atomically flat terraces is usually explained by the Prandtl-Tomlinson model [14,15]. In this framework, a point mass representing the tip apex is driven by a lateral spring across an effective potential U_{eff} . On alkali halide surfaces, the spring constant k almost coincides with the lateral stiffness of the contact area [10]. This quantity can be obtained from the analysis of friction loops [16,17], and in our case it turns out to be $\sim 1 \text{ N/m}$. On a flat terrace, long-range interactions can be neglected and the potential

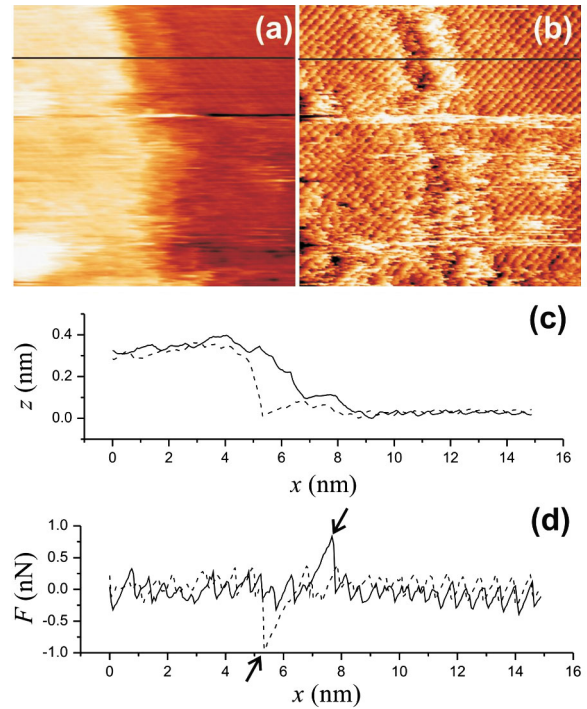


FIG. 2 (color online). (a) Topography and (b) lateral force images acquired in the same conditions as in Fig. 1 after prolonged scanning at high load. Profiles are taken along the black line for (c) the topography and (d) the lateral force (continuous curves). The dashed profiles represent the backward scan direction (images not shown). Note that friction increases at the step edge for both the step-up direction and the step-down direction (see arrows).

U_{eff} corresponds to the potential U_{int} describing the chemical interaction between the atoms at the bottom of the tip and surface atoms. The potential U_{int} has thus the periodicity of the surface lattice a . In the presence of a step edge, however, long-range interactions are varying, meaning that a second contribution U_{long} to the tip-surface potential has to be taken into account. Our experimental results suggest that the potential U_{long} is highly sensitive to the distribution of the atoms at the tip apex.

In order to quantify the effective potential U_{eff} , we have calculated the Lennard-Jones (LJ) contribution U_{LJ} to the effective potential in the case of a single atom crossing a monatomic step edge on NaCl(001) (Fig. 3). The calculation of the LJ potential was done analogously as in the paper by Hölscher, Ebeling, and Schwarz [5] with the parameters $E_0 = 1 \text{ eV}$ and $r_0 = 0.56 \text{ nm}$. In order to reproduce the feedback mechanism of the AFM, the atom was first set at a certain distance d from the surface and then forced to travel along the curves $\partial U_{\text{LJ}}/\partial z = \text{const}$. As shown in Figs. 3(a) and 3(b), the LJ potential suddenly drops at the step edge and slowly recovers over a distance on the order of two lattice constants. The potential drop is anticipated by an energy barrier. When $d = 0.65 \text{ nm}$, the depth E_1 of the potential well is larger than the height E_2 of

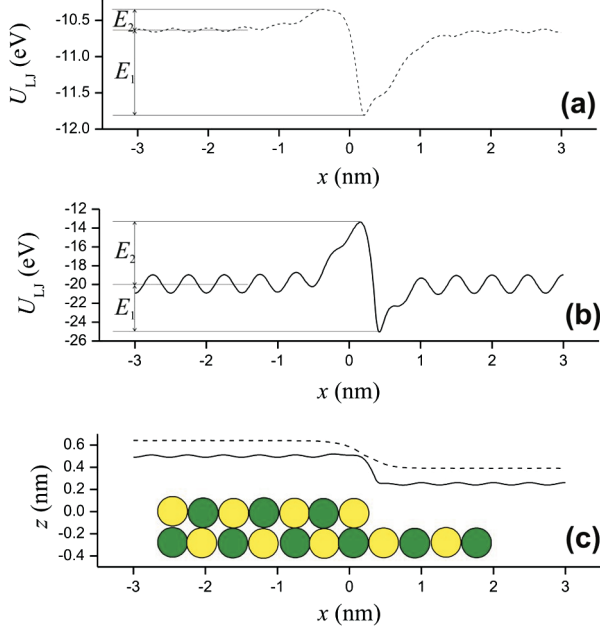


FIG. 3 (color online). Lennard-Jones potential calculated at constant load starting from a distance (a) $d = 0.65$ nm and (b) $d = 0.55$ nm from a stepped NaCl(001) surface. (c) Corresponding tip trajectories when $d = 0.65$ nm (dashed curve) and $d = 0.55$ nm (continuous curve).

the energy barrier [Fig. 3(a)]. However, when the surface is approached, the quantity E_2 increases faster than E_1 and $E_2 > E_1$ when $d = 0.55$ nm [Fig. 3(b)]. The electrostatic potential U_{el} follows the atomic corrugation of the NaCl (001) surface, with a slight enhancement at the step edge. At the distances considered in Fig. 3, its contribution to the potential U_{eff} is 1 order of magnitude less than that of the LJ potential and can be safely ignored in the rest of the discussion.

It is reasonable to assume that the energy landscape sensed by the sharp tip used in the experiment, which was close to jump-off, has similar features as the LJ calculation in Fig. 3(a). In order to prove that, we have constructed an empirical one-dimensional potential $U_{eff}(x)$ formed by (i) a sinusoid representing the periodic interaction U_{int} between tip and surface and (ii) an asymmetric well simulating a sharp drop followed by a slow recovery of the potential U_{long} :

$$U_{long}(x) = E_1 \left[-\operatorname{erf}\left(\frac{x}{b_1}\right) + \operatorname{erf}\left(\frac{x-c}{b_2}\right) \right]. \quad (1)$$

In Eq. (1), the parameters b_1 , b_2 ($> b_1$), and c are expected to be in the order of the tip apex, and the origin of the x coordinates corresponds to the step edge. Finally, we have calculated the lateral force F experienced by a point mass driven by a spring with elastic constant $k = 1$ N/m over the potential U_{eff} under adiabatic conditions, i.e., neglecting the inertia and the damping of the point mass. As shown in Fig. 4(a), we find that a decay of U_{long} on

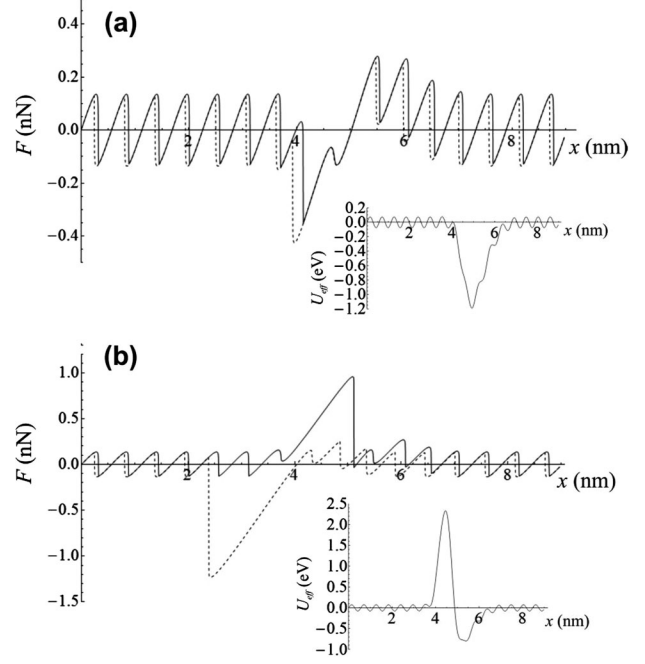


FIG. 4. Friction response of a point mass driven by an elastic spring across the potential $U_{eff} = U_{int} + U_{long}$. The potential U_{int} follows the crystal lattice with a corrugation of 0.1 eV, whereas U_{long} is represented (a) by the asymmetric potential well (1) with $E_1 = 0.8$ eV, $b_1 = 0.40$ nm, and $b_2 = c = 0.90$ nm and (b) by the same potential well anticipated by a Gaussian peak with a height of 2.3 eV. The corresponding shapes of U_{eff} are shown in the two insets.

the order of 1 eV and a corrugation of 0.1 eV for the potential U_{int} are consistent with the experimental results in Fig. 1.

A different situation is expected for the blunt tip. In this case, while the fore atoms at the tip apex cross the step edge, the tip-surface interaction decreases and the tip is pushed down by the feedback mechanism of the AFM. However, the back atoms of the apex are still in contact with the upper terrace, which leads to a strong repulsive effect [the energy barrier in Fig. 3(b)]. Only when the tip has crossed a distance corresponding to the apex width does the repulsive effect end, and atomic stick-slip continues on the lower terrace. This can be reproduced by adding a Gaussian profile to the potential U_{long} used for the sharp tip. The choice of a Gaussian shape is motivated by our ignorance of the atomic arrangement at the tip apex. To take into account the finiteness of the apex, we have also assumed that the barrier is found at locations separated by a few lattice constants when scanning forward and backward. A good agreement with the results in Fig. 2 is obtained by assuming that the barrier has a height of 2.3 eV and the separation between forward and backward scans is 4 times the lattice constant [Fig. 4(b)].

Our conclusions differ from previous works in the literature, where friction at step edges was associated with

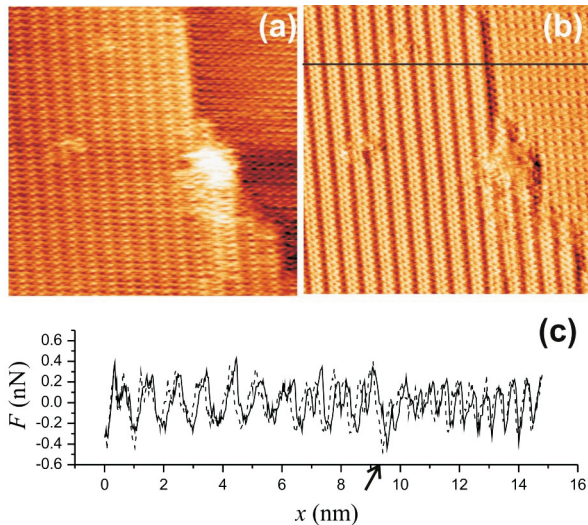


FIG. 5 (color online). (a) Topography image (frame size: $15 \times 15 \text{ nm}^2$), (b) friction map, and (c) corresponding friction loop acquired while scanning a Ge(001) surface with a normal force $F_N = -3 \text{ nN}$. The probing tip crosses a step edge at $x = 9.5 \text{ nm}$ (see arrow). The step height is approximately 0.25 nm .

the presence of a Schwöbel-Ehrlich barrier. Our results show that this is the case only for a blunt tip, where a strong repulsion between part of the tip apex and surface atoms is unavoidable, as confirmed by the occurrence of abrasion wear. An atomically sharp tip, however, can slide across the step edge without experiencing an activation barrier and wearing off the surface. Applying a low load (close to the jump-off) is enough to reach this goal. At this point the question may arise whether these results are limited to ionic crystal surfaces or they are more general. To address this point we have also measured the lateral force across a monatomic step edge on a semiconducting Ge(001) surface. The frictional response of a sharp silicon tip in the two directions is indeed very similar to the case of NaCl(001) (Fig. 5). This gives a strong indication that the removal of the Schwöbel barrier predicted in the calculation of the LJ potential is a general effect. The same cannot be said for the occurrence of abrasive wear when the tip is blunt and/or the normal load is increased. Already in the case of NaCl systematic measurements performed by Sheehan across a step edge showed that the wear rate is strongly dependent on the humidity conditions [18]. Wear is enhanced when relative humidity is $< 20\%$, which makes it an important issue in UHV measurements. In order to gain further insight into this topic, atomistic simulations of friction with finite tips become mandatory. An example was recently given by Wyder *et al.*, who simulated the atomic stick-slip experienced by differently shaped tips sliding on flat KBr surfaces [19]. An extension of these studies to stepped surfaces is still missing to our knowledge.

In summary, we have measured friction across step edges by using an AFM tip in a sharp and a blunt condition. In the first case, a well-defined stick-slip motion is observed at the step edge, with a jump length corresponding to the tip width. The configuration of the tip and cantilever with respect to the surface are quite similar while scanning up and down the step edge. This leads to overlapping lateral force profiles and indicates that the lateral force is reduced at the step edge when scanning step-down. The sharpness of the tip facilitates scanning the step edge without occurrence of a Schwöbel-Ehrlich barrier (provided that the normal load is not too high). Contrary to that, a blunt tip acts as a pinning center, where the lateral force is increased also in the step-down direction as reported in previous experimental studies. The atomic features observed in the present investigation reveal that abrasion wear may occur in such a case.

This work was supported by the Swiss National Science Foundation and the Polish Ministry of Science and Higher Education (268/N-ESF/2008/0) within the projects “Active Control of Friction” (ACOF) and “Atomic Friction” (AFRI) of the ESF Program “Friction and Adhesion in Nanomechanical Systems” (FANAS). We also acknowledge the Swiss National Center of Competence in Research on Nanoscale Science for financial support, and we thank Professor Alexis Baratoff for stimulating discussions on the topic and Dr. Thilo Glatzel and Dr. Shigeki Kawai for technical assistance.

*Corresponding author.

- [1] G. Meyer and N.M. Amer, *Appl. Phys. Lett.* **57**, 2089 (1990).
- [2] J.A. Ruan and B. Bhushan, *J. Appl. Phys.* **76**, 8117 (1994).
- [3] E. Meyer *et al.*, *J. Vac. Sci. Technol. B* **14**, 1285 (1996).
- [4] T. Müller *et al.*, *Phys. Rev. Lett.* **79**, 5066 (1997).
- [5] H. Hölscher, D. Ebeling, and U.D. Schwarz, *Phys. Rev. Lett.* **101**, 246105 (2008).
- [6] R.L. Schwöbel and E.J. Shipsey, *J. Appl. Phys.* **37**, 3682 (1966).
- [7] G. Ehrlich, *J. Chem. Phys.* **44**, 1050 (1966).
- [8] L. Howald *et al.*, *Appl. Phys. Lett.* **63**, 117 (1993).
- [9] R. Lüthi *et al.*, *Surf. Sci.* **338**, 247 (1995).
- [10] A. Socoliuc *et al.*, *Phys. Rev. Lett.* **92**, 134301 (2004).
- [11] E. Gnecco, R. Bennewitz, and E. Meyer, *Phys. Rev. Lett.* **88**, 215501 (2002).
- [12] A. Socoliuc *et al.*, *Science* **313**, 207 (2006).
- [13] Z. Tshiprut, A.E. Filippov, and M. Urbakh, *Phys. Rev. Lett.* **95**, 016101 (2005).
- [14] L. Prandtl, *Z. Angew. Math. Mech.* **8**, 85 (1928).
- [15] G.A. Tomlinson, *Philos. Mag.* **7**, 905 (1929).
- [16] R.W. Carpick *et al.*, *Appl. Phys. Lett.* **70**, 1548 (1997).
- [17] M.A. Lantz *et al.*, *Phys. Rev. B* **55**, 10776 (1997).
- [18] P.E. Sheehan, *Chem. Phys. Lett.* **410**, 151 (2005).
- [19] U. Wyder *et al.*, *J. Vac. Sci. Technol. B* **25**, 1547 (2007).